THE JOURNAL OF BIOLOGICAL CHEMISTRY
Vol. 280, No. 20, Issue of May 20, pp. 19852–19857, 2005
Printed in U.S.A.

The Fusion Activity of HIV-1 gp41 Depends on Interhelical Interactions*

Received for publication, February 25, 2005
Published, JBC Papers in Press, March 16, 2005, DOI 10.1074/jbc.M502196200

Tara R. Suntoke‡§¶ and David C. Chan‡‖

From the ‡Division of Biology, California Institute of Technology, Pasadena, California 91125 and the §Division of Biology, Massachusetts Institute of Technology, Cambridge, Massachusetts 02139

Infection by human immunodeficiency virus type I requires the fusogenic activity of gp41, the transmembrane subunit of the viral envelope protein. Crystallographic studies have revealed that fusion-active gp41 is a "trimer-of-hairpins" in which three central N-terminal helices form a trimeric coiled coil surrounded by three antiparallel C-terminal helices. This structure is stabilized primarily by hydrophobic, interhelical interactions, and several critical contacts are made between residues that form a deep cavity in the N-terminal trimer and the C-helix residues that pack into this cavity. In addition, the trimer-of-hairpins structure has an extensive network of hydrogen bonds within a conserved glutamine-rich layer of poorly understood function. Formation of the trimer-of-hairpins structure is thought to directly force the viral and target membranes together, resulting in membrane fusion and viral entry. We test this hypothesis by constructing four series of gp41 mutants with disrupted interactions between the N- and C-helices. Notably, in the three series containing mutations within the cavity, gp41 activity correlates well with the stability of the N-C interhelical interaction. In contrast, a fourth series of mutants involving the glutamine layer residue Gln-653 show fusion defects even though the stability of the hairpin is close to wild-type. These results provide evidence that gp41 hairpin stability is critical for mediating fusion and suggest a novel role for the glutamine layer in gp41 function.

Structural analyses of the transmembrane subunits of several viral envelope proteins (Env)[1] have provided much insight into the mechanism of Env-mediated membrane fusion. Remarkably, the putative fusion-active structures of these proteins from retroviruses (*e.g.* HIV, simian immunodeficiency virus, and Moloney murine leukemia virus), orthomyxoviruses (influenza), paramyxoviruses (simian virus type 5 and human respiratory syncytial virus), filoviruses (Ebola), and coronaviruses (severe acute respiratory syndrome-associated coronavirus) (1, 2) all reveal the same six-helix bundle conformation. This six-helix structure can also be described as a trimer-of-hairpins in which each hairpin consists of an N-terminal helix (N-helix) packed against an antiparallel C-terminal helix (C-helix). Three central N-helices form a coiled coil surface with three prominent hydrophobic grooves that each allow C-helix binding (3–6). Thus, the trimer-of-hairpins structure is largely stabilized by hydrophobic packing between the three internal N-helices and between the N- and C-helices (Fig. 1, *A* and *B*). This fusion-active configuration juxtaposes the amino terminus of gp41, which contains a fusion peptide inserted into the target cell membrane, with the carboxyl terminus, which contains the transmembrane anchor in the viral membrane. The current model for membrane fusion proposes that formation of the hairpin structure provides the energy necessary for viral and cellular membrane apposition, leading to membrane fusion (1, 3, 6).

There are two prominent features of the trimer-of-hairpins structure in HIV and simian immunodeficiency virus gp41. First, three symmetric hydrophobic cavities on the surface of the N-helix coiled coil each forms a docking site for three residues from a C-helix. Notably, small peptides or synthetic molecules targeted to these cavities prevent trimer-of-hairpins formation and inhibit fusion (7, 8); the efficacy of these molecules underscores the critical role of interhelical interactions within the cavity in gp41 function. Second, a planar cluster of conserved glutamine and asparagine residues, from both the N- and C-helices, form a hydrogen-bonded layer within the six-helix bundle (5, 6, 9). Though a novel structural feature, the function of this "glutamine layer" remains unclear (6, 9); indeed, none of the reported mutations in this region reduce gp41 activity. In fact, such substitutions can increase gp41 core stability (10–12) and, in the unusual case of a Gln-652 to leucine mutation (Q652L), appear to increase fusogenicity (13).

Several mutational and biophysical analyses of gp41 support the hypothesis that hairpin formation provides the driving force for membrane fusion. For example, the N-helix residues Leu-565, Leu-568, and Val-570, located on the cavity surface, form hydrophobic contacts with C-helices as determined by x-ray crystallography. Alanine mutations at these positions decrease six-helix bundle stability and reduce envelope-mediated fusion (12–16). These mutations are notable, because they likely represent a specific defect in the fusion pathway, unlike some N- and C-helix mutants that fail to correctly process the gp160 precursor into gp120 (the receptor binding subunit) and gp41 (11, 12, 16). Although these studies support a role for hairpin formation in membrane fusion, a systematic analysis of the correlation between hairpin stability and gp41 activity would provide a more rigorous test of the model.

In this study we seek to identify the energetic contribution of the N-C helical interaction to the fusion reaction. We made a series of substitutions at each of four positions in the N-C

* This work was supported in part by National Institutes of Health Grant PO1 GM56552. The costs of publication of this article were defrayed in part by the payment of page charges. This article must therefore be hereby marked "*advertisement*" in accordance with 18 U.S.C. Section 1734 solely to indicate this fact.

¶ Supported by the Massachusetts Institute of Technology and Merck Pharmaceuticals.

‖ To whom correspondence should be addressed: Division of Biology, MC 114-96, 1200 E. California Blvd., Pasadena, CA 91125. Tel.: 626-395-2670; Fax: 626-395-8826; E-mail: dchan@caltech.edu.

[1] The abbreviations used are: Env, envelope glycoprotein; CD, circular dichroism; C-helix, C-terminal heptad repeat region of gp41; HIS, hexahistidine tag; HIV-1, human immunodeficiency virus type 1; N-helix, N-terminal heptad repeat region of gp41; PBS, phosphate-buffered saline; SNARE, soluble *N*-ethylmaleimide-sensitive factor attachment protein receptor.

helical interface. We report that for mutations within the N-helix cavity, the fusion activity of gp41 depends on the stability of the N-C interface. In contrast, for the series of substitutions in the glutamine layer, we find that gp41 activity is abolished even in the presence of stable N-C interactions, thereby providing evidence for an important role for the glutamine layer in gp41-mediated fusion.

MATERIALS AND METHODS

Plasmid Construction and Mutagenesis—Env mutations were made using QuikChange site-directed mutagenesis (Stratagene) of pBS-SKII containing HXB2 gp160 (pBS-SKII-gp160) and verified by DNA sequencing. For expression in 293T cells, all mutations were subcloned into pcDNA1.1/Amp (Invitrogen). For generation of stable cell lines, the mutations were subcloned into the pB-IRES-CD2 retroviral vector (gift from Jonathan Bogan, Whitehead Institute, Cambridge MA).

For expression of recombinant proteins, mutations were cloned into the pAED4 vector (4). Mutant N34 and wild-type C28 fragments were PCR-amplified from pBS-SKII-gp160 using the primers 5′-GCAATTC-CATATGTCTGGTATAGTGCAGCAG-3′ (N34 forward) and 5′-ACCGC-GACCACCGCTTCTTGCTTGGAGCTGCTTG-3′ (L6N34 reverse) for the N34 fragment and 5′-GGTGGTCGCGGTGGTTGGATGGAGTGG-GACAGAG-3′ (L6C28 forward) and 5′-GGAATTCCTAGTGATGAT-GATGATGATGCTTTTCTTGCTGGTTTTGC-3′ (C28-HIS reverse) for the C28 fragment. These primers introduce a six-residue linker (Ser-Gly-Gly-Arg-Gly-Gly) between N34 and C28 and a hexahistidine tag (HIS) 3′ of C28. For mutant C28 fragments, C28-HIS reverse primers encoding the mutations were used. The N and C fragments were joined by overlap PCR with primers N34 forward and C28-HIS reverse and subcloned into pAED4.

Protein Expression and Purification—Bacterial cultures expressing N34(L6)C28-HIS variants were induced with 1 mM isopropyl-1-thio-β-D-galactopyranoside for 3–4 h. Cell pellets were resuspended in lysis buffer (50 mM Tris (pH 8), 15% glycerol, and 300 mM NaCl) containing 10 μM $MgCl_2$, 1 μM $MnCl_2$, and 100 μg/ml DNase I, lysed by sonication, and centrifuged (27,000 × *g* for 30 min) to separate the soluble and inclusion body fractions. The pellet was washed again in lysis buffer, and supernatants from both washes were pooled. With the exception of the glycine mutants, all peptides were present in the soluble fraction and affinity-purified using nickel-nitrilotriacetic acid (Qiagen, Inc.). For the glycine mutants, inclusion body pellets were solubilized in lysis buffer containing 6 M guanidine-HCl before purification using nickel-nitrilotriacetic acid beads. Peptide-containing fractions were dialyzed into 5% acetic acid, purified to >95% purity over a preparative C5 column by reverse-phase high performance liquid chromatography, and lyophilized.

Circular Dichroism (CD) Spectroscopy—Lyophilized peptide was dissolved in water, and concentrations were determined by absorbance at 280 nm in 6 M guanidine-HCl (17). Peptides were then diluted to 10 μM in PBS (50 mM sodium phosphate and 150 mM sodium chloride (pH 7)). CD spectra were obtained on an AVIV 62DS CD spectrometer. To determine helical content, a value of −33,000 degree cm^2 $dmol^{-1}$ was used for theoretical 100% helicity (12). Thermal denaturation scans were performed on 10 μM peptide samples in PBS. The midpoint of the thermal unfolding transition (T_m) was calculated as the maximum value of the first derivative of the molar ellipticity at 222 nm ($[\theta]_{222}$) with respect to temperature. Consistent with previous reports for N34(L6)C28 (10, 11), thermal denaturation of these recombinant peptides was cooperative but not reversible.

Sedimentation Equilibrium—All measurements were recorded on a Beckman XL-I analytical ultracentrifuge with a Ti-60a rotor. Wild-type N34(L6)C28-HIS was dialyzed overnight in PBS or sodium acetate buffer (50 mM sodium acetate and 150 mM NaCl (pH 5.5)), and diluted to 5, 10, and 30 μM. Samples dialyzed in PBS formed some precipitate, whereas samples in sodium acetate remained fully soluble. Data were collected at 20 °C with rotor speeds of 20, 30, and 42 krpm and wavelengths of 229 and 280 nm. Data sets were fitted simultaneously with WinNonlin (version 1.06) (18). No systematic residuals were observed, and both samples fit well to a single species model.

Because wild-type N34(L6)C28-HIS formed stable trimers in both buffers and remained fully soluble after overnight dialysis at low pH, mutant peptides were analyzed in the sodium acetate buffer. All N34(L6)C28-HIS variants except L565G fit best to a single species model, showed no systematic residuals, and had molecular weights within 10% of those calculated for an ideal trimer. The L565G peptide was predominantly trimeric in solution, but the data fit slightly better as a monomer-trimer equilibrium containing 80% trimers.

Envelope Glycoprotein Expression and Western Blot Analysis—Mutant envelope glycoproteins were expressed in 293T cells by transient transfection for expression analysis and cell-cell fusion assays. 293T cells were plated in gelatin-coated 12-well plates. At ~30–50% confluency, cells were transfected with 800 ng of pcDNA-gp160 expressing mutant gp160 and 400 ng of pnGFP (a plasmid expressing nuclear green fluorescent protein) using Lipofectamine 2000 (Invitrogen). Transfection efficiency was assessed by green fluorescent protein fluorescence and was similar for all mutants (~30–50%).

Envelope expression was measured by Western blot analysis. gp41 and gp160 from cell lysates were analyzed with an anti-gp41 monoclonal antibody, Chessie 8 (National Institutes of Health AIDS Research and Reference Reagent Program). Shed gp120 was immunoprecipitated from the culture supernatant using an anti-gp120 polyclonal antibody (gift of Peter Kim, Merck Research Laboratories, West Point PA), and protein-A-Sepharose beads (Sigma). To determine cell surface expression levels of Env, transfected cells were washed with cold PBS (pH 8.0) and biotinylated using 5 mM sulfosuccinimidyl-6-(biotinamido)hexanoate (Pierce) in PBS for 30 min at 4 °C. After washing with PBS containing 100 mM glycine to remove excess biotin, cells were lysed in PBS containing 1% Nonidet P-40 (Sigma). Biotinylated surface proteins were precipitated using immobilized NeutrAvidin (Pierce) and separated by SDS-PAGE.

Stable cell lines expressing the alanine mutants were made using retroviral transduction of NIH3T3 cells. To generate retrovirus, 293T cells were plated on gelatin-coated 60-mm plates and transfected with pBI-CD2-gp160 encoding mutant gp160 and a Moloney murine leukemia virus packaging vector, pCLeco (gift from C. Lois, Massachusetts Institute of Technology). A 1:2 dilution of viral supernatant was used to infect NIH3T3 cells in the presence of 4 μg/ml polybrene. After several passages, the infected NIH3T3 cell lines were used for dye transfer assays.

Cell-Cell Fusion Assay—Forty-eight hours after transient transfection, 293T cell monolayers were resuspended and counted. A mixture of 4×10^4 envelope-expressing 293T cells and 4×10^4 target cells, 3T3-T4-CXCR4 (National Institutes of Health AIDS Research and Reference Reagent Program), was plated in duplicate into gelatin-coated, eight-well slides and incubated for 21 h at 37 °C. After fixation and hematoxylin staining, the number of syncytia per well was counted under phase microscopy. Cells containing three or more nuclei were scored as syncytia.

Dye Transfer Fusion Assay—3T3 cells stably expressing gp41 mutations were plated at a density of 1×10^6 cells per 60-mm dish. Eight hours later, cell monolayers were incubated with 420 nM calcein-AM (Molecular Probes) in PBS for 10 min at 37 °C and gently washed twice with PBS before the addition of labeled target cells. Target cells, 3T3-T4-CXCR4, were labeled with the lipid dye octadecyl rhodamine B (R18) (Molecular Probes). 2×10^6 target cells were washed in PBS, incubated in PBS containing 2 μM R18 for 15 min at room temperature in the dark, and washed twice in PBS before resuspension in growth media. Approximately 4×10^5 target cells were added to envelope-expressing monolayers, and dishes were immediately incubated at 37 °C. Cells were examined for dye transfer every 20–30 min by counting the number of co-labeled cells in five separate fields at 200× magnification.

RESULTS

Design of Four Allelic Series—Residues Leu-565, Leu-568, and Val-570 are located on the surface of the N-terminal coiled coil within a large cavity and interact with the internal face of the C-helix (Fig. 1, *A* and *B*). In previous studies, mutation of these residues to alanine reduced fusion but did not affect gp160 processing or gp120-gp41 association (12–15), suggesting a specific defect in the fusion pathway. To obtain a range of gp41 core stabilities, each position was mutated to glycine, alanine, and phenylalanine. We chose glycine for its helix-destabilizing properties (19), alanine for its reduced hydrophobic bulk, and phenylalanine for its increased bulk over the native leucine or valine residue.

The polar contacts within the glutamine layer were disrupted by mutagenesis of Gln-653 (Fig. 1*C*). This residue is buried in the interhelical interface and forms hydrogen bonds with neighboring helices in the core crystal structure (6, 20). Furthermore, it is highly conserved; only two of 630 viruses in the Los Alamos HIV sequence data base show mutations at this position (www.hiv.lanl.gov). The Q653A and Q653L substitu-

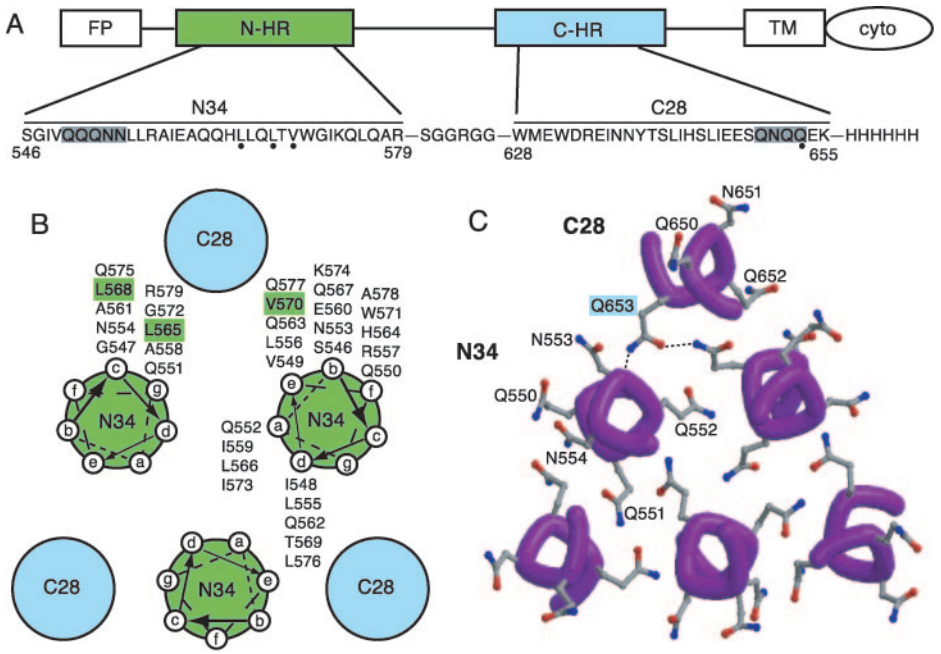

FIG. 1. **Structure of the HIV-1 gp41 core.** *A*, a schematic diagram of HIV-1 HXB2 gp41. Important functional domains include the fusion peptide (*FP*), N- and C-terminal heptad repeats (*N-HR* and *C-HR*), transmembrane domain (*TM*), and the cytoplasmic tail (*cyto*). The sequence of the recombinant peptide N34(L6)C28-HIS containing the N-terminal heptad repeat residues 546–579, a six residue linker, C-terminal heptad repeat residues 628–655, and a C-terminal hexahistidine tag is shown below. Residues are numbered according to their positions in HXB2 gp160. *Dots* below specific amino acids indicate residues that are mutated in this study, and *highlighted* glutamine and asparagine residues denote amino acids within the glutamine layer. *B*, helical wheel representation of N34 and C28. Residues at the *a* and *d* positions of the N-helices interact to form the interior of the trimeric coiled coil. C-terminal helices pack against the grooves between adjacent N-terminal helices. N-HR residues that are mutated in this study are *highlighted in green*. *C*, the glutamine layer of HIV-1 gp41. A cross-section of the gp41 core reveals glutamine and asparagine residues from both the N-terminal and C-terminal heptad repeat domains that form an interconnected polar layer. The C-helix residue Gln-653 protrudes toward the center of the six-helix bundle and is intimately involved in the polar network. Crystallographic studies suggest that this side chain in both HIV and the simian immunodeficiency virus forms hydrogen bonds with the backbone and a glutamine residue on adjacent N-helices (6, 20). These putative hydrogen bonds are shown as *dashed lines*. Residues in *panels B* and *C* are denoted using single letter amino acid abbreviations with position numbers.

tions were designed to abolish polar contacts with neighboring glutamine residues, whereas the Q653E substitution retains bulk and polarity.

Biophysical Analysis of Recombinant gp41 Core Structures—We used a recombinant peptide model to measure the biophysical properties of mutant gp41 cores. This gp41 core peptide, termed N34(L6)C28-HIS, contains N- and C-terminal helices that are joined by a six residue linker (Fig. 1*A*). It is similar to the previously described N34(L6)C28 peptide (21) but contains a C-terminal HIS tag to facilitate purification. Circular dichroism indicates that the molecule is >90% helical and thermostable, with a T_m of 74 °C. In addition, it forms a discretely trimeric species as determined by sedimentation equilibrium (Fig. 2 and Table I). When compared with published data for N34(L6)C28, N34(L6)C28-HIS has a 4 °C higher melting temperature. We speculate that addition of the C-terminal tag promotes stability by attenuating the helix dipole moment or by reducing fraying of the helical ends (19, 22).

For the three mutant series involving the N-helix, biophysical analysis indicated that we successfully generated a wide range of stabilities in the gp41 core (Table I). In each position, all mutants are less stable than wild-type, with the relative order Gly < Ala < Phe < wild-type. At position 568 the phenylalanine mutant (T_m of 61 °C) is only slightly more stable than the alanine mutant (T_m of 60 °C). The low stability of the L568F variant may be caused by local distortion to accommodate the large aromatic ring. All mutants are highly helical, and, with the exception of L565G (see "Materials and Methods"), the least thermostable variant in this study, all form clean trimers as evidenced by sedimentation equilibrium analysis (Table I).

Interestingly, mutations at Gln-653 do not appreciably destabilize the six-helix bundle structure. The Q653A, Q653L, and Q653E mutants have T_m values close to that of wild-type and form stable trimers (Table I). Thus, in contrast to the effects observed with the cavity mutations, altering the native interhelical interaction within the glutamine layer does not substantially affect gp41 core stability.

Expression and Processing of gp41 Variants—We examined the expression and processing of envelope mutants after transient transfection of mutant constructs into 293T cells. Transfection efficiency, assessed by co-transfection of a green fluorescent protein expression vector, was similar for all Env proteins.[2] Western blot analysis of the cell lysates with an anti-gp41 monoclonal antibody reveals that all gp41 mutants, except L565A, are expressed and processed at levels similar to that of wild-type (Fig. 3, *A* and *B*). These results are quantitated by gel densitometry in Table II and are consistently similar to wild-type levels (80–120%). L565A gp41 is expressed at 60% of wild-type. The levels of cell surface Env were quantitated by surface biotinylation and precipitation using avidin-conjugated beads. Expression levels of mutant gp160 and gp41 on the cell surface were similar to that of wild-type (data not shown), and the ratio of surface gp41 to gp160 confirmed that proteolytic processing of the Env precursor was normal for all mutants (Table II).

Under normal conditions, the noncovalent interaction between gp120 and gp41 is labile, and a portion of gp120 is shed from the surface of virions or Env-expressing cells. Some mu-

[2] T. R. Suntoke and D. Chan, unpublished data.

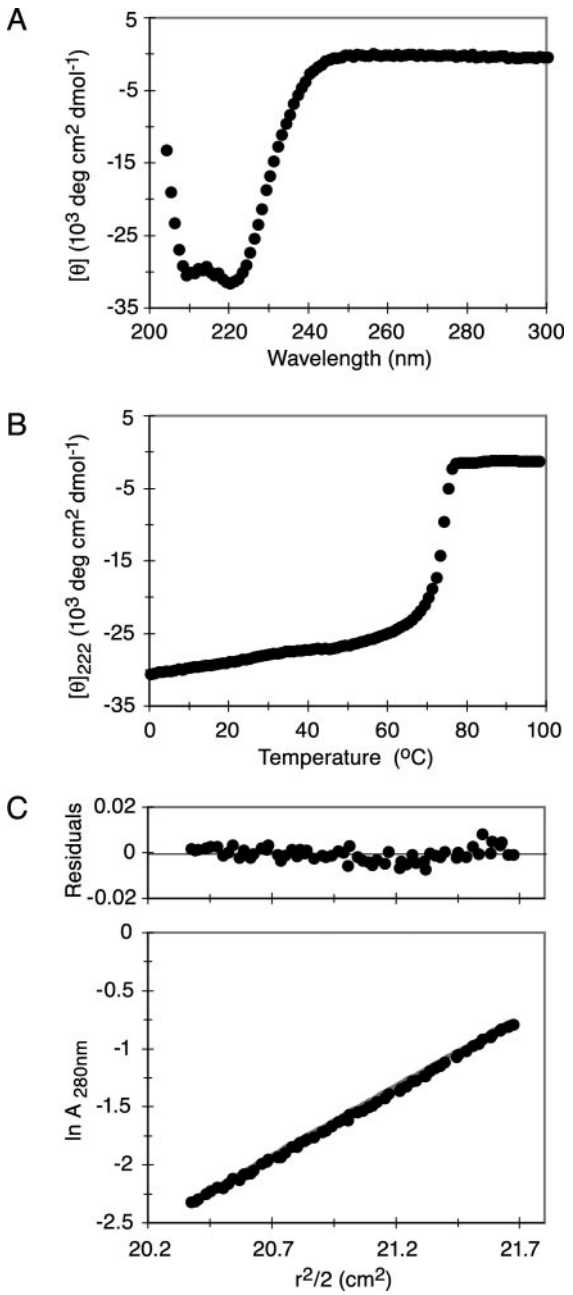

FIG. 2. **Biophysical properties of N34(L6)C28-HIS.** *A*, the CD spectra of N34(L6)C28-HIS (10 μM) in PBS at 0 °C. *B*, thermal dependence of the CD signal at 222 nm for a 10 μM peptide sample in PBS. *C*, representative sedimentation equilibrium data for N34(L6)C28-HIS (10 μM) in sodium acetate buffer collected at 20 krpm and 20 °C. The deviation of the data from the trimer model is plotted in the *top section*. The *bottom section* shows the data and a *line* representing the fit using an ideal single species model.

tations in gp41 affect its association with gp120, leading to the increased release of gp120 into the culture supernatant. Immunoprecipitation of gp120 from the culture medium followed by Western blot analysis shows that steady-state levels of shed gp120 are similar for wild-type and all mutants (Fig. 3 and Table II). These results further indicate that mutations at positions 565, 568, 570, and 653 in gp41 do not affect the native conformation of the envelope glycoprotein.

Fusogenic Potential of Mutant Envelope Glycoproteins—The gp41 mutants were tested for membrane fusion activity with syncytia assays. For the N-helix mutants, there is good correlation between thermostability of the gp41 core and fusion activity (Table II). The glycine mutants, which are the least

TABLE I
Summary of biophysical data for N34(L6)C28-HIS mutants

Mutant	$-[\theta]_{222}$ [a]	T_m [a]	M_{obs}/M_{calc} [b]
	10^3 deg cm^2 dmol^{-1}	°C	
N34(L6)C28-HIS	−30.9	74	2.8
L565G	−23.1	38	2.5
L565A	−24.2	57	2.7
L565F	−24.8	63	3.0
L568G	−25.8	43	2.9
L568A	−27.4	60	3.0
L568F	−23.0	61	2.8
V570G	−27.1	49	2.9
V570A	−27.0	62	3.1
V570F	−28.0	68	2.9
Q653A	−30.5	74	2.9
Q653L	−28.2	76	3.1
Q653E	−28.9	73	3.0

[a] All circular dichroism wavelength scans and thermal melts were performed on 10 μM peptide samples in PBS (pH 7.0).
[b] Sedimentation equilibrium results are shown as the ratio of observed molecular weight (M_{obs}) to calculated molecular weight for a monomer (M_{calc}).

stable, have barely detectable levels of fusion. As the stabilities of the mutants increase, there is a simultaneous increase in fusion activity. This trend becomes clear when the fusion activity of the mutants is plotted as a function of gp41 stability (Fig. 4). This plot also reveals that the V570A mutant has unusually low fusion activity. V570A has intermediate stability (T_m of 62 °C) that is comparable with that of L565F, L568A, and L568F; however, unlike these three mutants, it is severely deficient in cell fusion activity. The reason for this anomaly remains to be determined. Our results agree with and extend previously published data for alanine mutants at positions 565, 568, and 570 (12, 14–16), which suggest a similar correlation between fusion and core stability.

The Gln-653 mutants provide a striking exception to this correlation. Despite its highly stable core structure, the Q653E substitution caused a 32% decrease in gp41 fusion activity compared with wild-type. A more severe mutation, Q653L, which abolishes polarity, further decreased gp41 function (55% of wild-type), whereas removal of both polarity and bulk with the Q653A mutation almost completely abrogated fusion. These results provide the first evidence that disruption of polar contacts within the gp41 glutamine layer decreases envelope-mediated fusion. The low fusogenicity of these 653 mutants, despite their extremely thermostable core structures, implicates the glutamine layer in a novel role in gp41 function.

Fusion Kinetics of Alanine Mutants—In gp41-mediated fusion there is a significant lag time after mixing cells before the first fusion events are observed (23). This delay is thought to reflect the slow conformational changes that occur in the envelope protein during the fusion process. Our N-helix mutants likely show fusion defects because weakened N-C helical interactions reduce the efficiency of membrane apposition. Alternatively, it is possible that attenuated N-C helical interactions also cause a delay in membrane apposition, resulting in a kinetic defect. In this scenario, Env molecules would display kinetics of fusion slower than that of wild-type, leading to a delay in the onset of initial fusion events.

To test this possibility, the L565A, L568A, and V570A mutants were analyzed further. The alanine mutants were chosen because they display low but detectable levels of fusion. The kinetics of fusion at early time points was analyzed using 3T3 cell lines stably expressing L565A, L568A, and V570A mutant envelope glycoproteins. The alanine mutants displayed levels of expression and processing similar to wild-type and fusion phenotypes analogous to those seen with transient transfections (4% for L565A, 17% for L568A, and 2% for V570A).[2] Dye

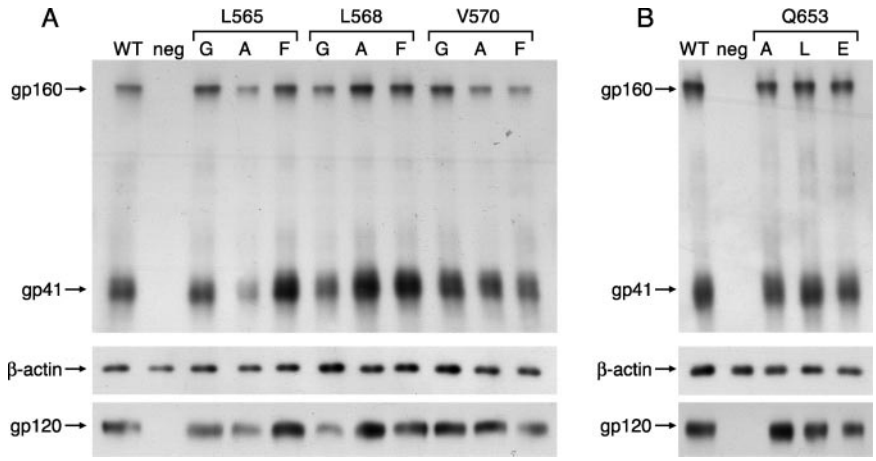

FIG. 3. **Expression and processing of mutant envelope glycoproteins.** *A*, expression analysis of N-helix mutant series. The *top section* shows cellular gp160 and gp41 levels detected by Western blot analysis, the *middle section* indicates the β-actin loading control, and the *lower section* depicts the amount of gp120 secreted into the culture medium. *B*, expression analysis of C-helix mutants at position 653. *Sections* are the same as in *panel A*. *WT*, wild-type; *neg*, empty vector-transfected.

TABLE II
Summary of Env expression, processing, and fusion

Env	gp160 expression[a]	gp41 expression[a]	Cell surface gp41/gp160[b]	gp120 secretion[c]	Cell-cell fusion[d]
					%
Wild-type	1.0	1.0	1.0	1.0	100 (± 7)
L565G	1.2	1.0	1.0	1.0	1 (± 0.1)
L565A	0.8	0.6	1.0	1.2	5 (± 0.6)
L565F	1.2	1.1	1.1	1.3	38 (± 3.1)
L568G	0.8	0.8	1.1	0.6	5 (± 0.6)
L568A	1.4	1.1	1.2	1.2	35 (± 2.3)
L568F	1.1	1.0	1.2	1.1	32 (± 1.4)
V570G	1.1	0.9	1.2	1.3	2 (± 0.2)
V570A	0.8	1.0	1.2	1.2	4 (± 0.1)
V570F	0.6	0.9	1.1	1.1	48 (± 2.7)
Q653A	1.0	1.1	0.8	1.3	7 (± 1.7)
Q653L	1.1	1.2	1.0	1.0	55 (± 6.1)
Q653E	1.1	1.1	0.9	1.1	68 (± 0.5)

[a] Relative Env expression was quantitated by densitometry. Cellular expression levels of gp160 or gp41 normalized to the amount of total protein in the lysate (β-actin) are shown.

[b] Env precursor processing is measured from cell surface proteins isolated by surface biotinylation and avidin precipitation. The reported number is the ratio (mutant gp41/mutant gp160)/(wt gp41/wt gp160), where wt stands for wild-type.

[c] The amount of shed gp120 (sgp120) is measured as the ratio (mutant sgp120/mutant cellular gp41)/(wt sgp120/wt cellular gp41), where wt stands for wild-type.

[d] To monitor cell-cell fusion activity, Env-expressing 293T cells were co-cultured with 3T3-T4-CXCR4 target cells for 21 hours at 37 °C. Following fixation and staining, fusion events were determined microscopically. Experiments were repeated in duplicate at least twice. The percentage of wild-type fusion in a representative fusion assay is shown. Numbers in parenthesis indicate S.D. The percent of fusion for cells transfected with a control vector lacking Env is 1.4 ± 0.7.

labeling of envelope-expressing cells with a cytosolic marker, calcein-AM, and target cells with a lipid marker, R18, allowed initial fusion events to be detected as dual-labeled cells. For each cell line, fusion was monitored approximately every 25 min. Fig. 5 shows the fusion progression of the alanine mutants at early time points after the co-incubation of effector and target cells. A small number of dye transfer events was initially detected for wild-type gp41 between 15 and 30 min post-mixing, followed by a dramatic increase starting at 80 min. These results correspond well with reported fusion kinetics experiments in which initial fusion events are detected after time lag, followed by rapid acceleration (Ref. 23 and references therein). With the alanine mutants it is difficult to reliably measure the onset of initial fusion events due to the low efficiency of fusion. Nevertheless, the acceleration phase for all the alanine mutants occurs between 80 and 100 min, indicating that the early kinetics for wild-type and mutant cell lines are similar.

DISCUSSION

Structural studies of the HIV-1 envelope protein suggest an elegant mechanism through which gp41 mediates apposition of viral and target cell membranes: the interaction of N- and C-helices to form the six-helix bundle forces the target cell membrane (containing the inserted fusion peptide) close to the viral membrane (containing the gp41 transmembrane segment). If this model is correct, the efficiency of gp41-mediated membrane fusion should depend on the strength of the N-C interhelical interaction. Indeed, with three sets of N-helix mutants we observe a strong correlation between trimer-of-hairpins stability and membrane fusion (Fig. 4). Fusion activities decrease rapidly with decreased stability, and all mutants with a T_m of 57 °C or lower lack significant activity, suggesting that there may be a threshold stability necessary to mediate membrane apposition. To further test this model, it will be important to develop experimental systems to directly measure the free energy change during the transition of gp41 from its native conformation to its fusogenic conformation.

Our fourth mutant series at C-helix position 653 shows markedly different results and suggests a significant role of the glutamine layer in gp41 function. Substitutions at position 653 do not significantly destabilize the hairpin but nevertheless reduce gp41-mediated membrane fusion (Tables I and II). Although the unusual structural features of the glutamine layer were noted in earlier structural studies (5, 6, 9), this is the first evidence of a functional role for this domain in membrane fusion.

The basis for the glutamine layer requirement remains to be elucidated. Previous mutations in this region have not supported an essential role for this region in membrane fusion

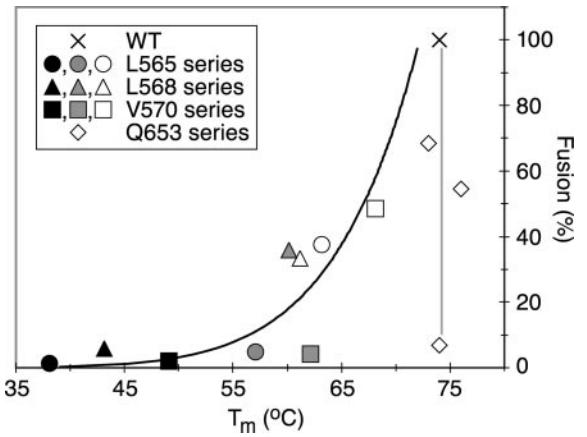

FIG. 4. **Correlation between gp41 core melting temperature and mutant fusion activity.** The N-helix mutants are shown as *circles* (Leu-565 (*L565*) series), *triangles* (Leu-568 (*L568*) series), and *squares* (Val-570 (*V570*) series). For these mutants the *symbols* are *black* for glycine mutants, *shaded* for alanine mutants, and *empty* for phenylalanine mutants. The Gln-653 (*Q653*) series is shown as *empty diamonds*, and wild-type (*WT*) is marked with an *X*. The N- and C-helix mutant series are each connected by a *line* showing the correlation between T_m and fusion.

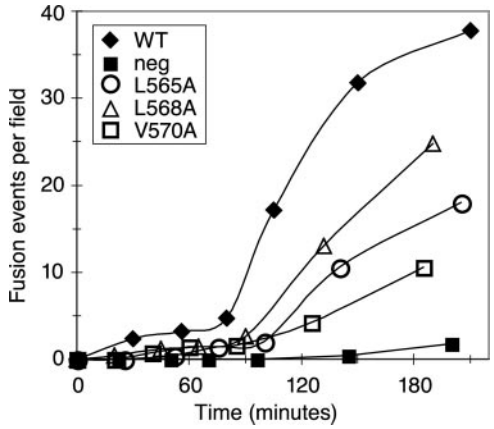

FIG. 5. **Fusion kinetics of N-helix alanine mutants.** 3T3 cell lines stably expressing envelope glycoprotein as well as an empty vector control were labeled with the cytosolic dye calcein-AM. Target cells (3T3-T4-CXCR4) were labeled with the lipid dye R18. Following co-culture at 37 °C, fusion events were detected as dual-labeled cells and counted over a 3-h time course. The fusion kinetics of wild-type (*WT*; *filled diamonds*), L565A (*open circles*), L568A (*open triangles*), V570A (*open squares*), and empty vector-transfected (*neg*; *filled squares*) cells are shown.

(10–13). Interestingly, in the N-helix, residues contributing to the glutamine layer are part of a small region implicated in resistance to the potent viral entry inhibitor enfuvirtide (reviewed in Ref. 24) (25). Viruses containing such mutations have reduced replicative fitness *in vitro* and revert back to wild-type in the absence of inhibitor (25, 26). In addition, SNARE helical bundles involved in intracellular vesicle fusion appear to have a similar ionic layer, which may be important for efficient recycling of SNARE complexes (27).

Numerous studies using designed coiled coils suggest that buried polar residues can play important roles in interhelical interactions. For instance, a buried glutamine can decrease the strength of interaction between helices (28). In addition, a buried polar residue at the interface of a short dimeric coiled coil can influence the orientation of the dimer, facilitating reversibility of assembly (29); this destabilization could permit the exchange of binding partners and may be biologically relevant. Although our Gln-653 mutations do not significantly change the stability or the oligomeric state of the gp41 core, it remains to be determined whether they have more subtle effects on gp41 protein structure.

Acknowledgments—We thank Drs. R. Olsen and A. Herr for assistance with the sedimentation equilibrium experiments, Dr. J. Kaiser for help with Fig. 1*C*, Drs. D. Eckert and M. Kay for critical review of the manuscript, and E. Griffin and members of the Chan lab for helpful discussions.

REFERENCES

1. Eckert, D. M., and Kim, P. S. (2001) *Annu. Rev. Biochem.* **70,** 777–810
2. Xu, Y., Lou, Z., Liu, Y., Pang, H., Tien, P., Gao, G. F., and Rao, Z. (2004) *J. Biol. Chem.* **279,** 49414–49419
3. Chan, D. C., Fass, D., Berger, J. M., and Kim, P. S. (1997) *Cell* **89,** 263–273
4. Lu, M., Blacklow, S. C., and Kim, P. S. (1995) *Nat. Struct. Biol.* **2,** 1075–1082
5. Tan, K., Liu, J., Wang, J., Shen, S., and Lu, M. (1997) *Proc. Natl. Acad. Sci. U. S. A.* **94,** 12303–12308
6. Weissenhorn, W., Dessen, A., Harrison, S. C., Skehel, J. J., and Wiley, D. C. (1997) *Nature* **387,** 426–430
7. Eckert, D. M., Malashkevich, V. N., Hong, L. H., Carr, P. A., and Kim, P. S. (1999) *Cell* **99,** 103–115
8. Ferrer, M., Kapoor, T. M., Strassmaier, T., Weissenhorn, W., Skehel, J. J., Oprian, D., Schreiber, S. L., Wiley, D. C., and Harrison, S. C. (1999) *Nat. Struct. Biol.* **6,** 953–960
9. Malashkevich, V. N., Chan, D. C., Chutkowski, C. T., and Kim, P. S. (1998) *Proc. Natl. Acad. Sci. U. S. A.* **95,** 9134–9139
10. Shu, W., Liu, J., Ji, H., Radigen, L., Jiang, S., and Lu, M. (2000) *Biochemistry* **39,** 1634–1642
11. Wang, S., York, J., Shu, W., Stoller, M. O., Nunberg, J. H., and Lu, M. (2002) *Biochemistry* **41,** 7283–7292
12. Lu, M., Stoller, M. O., Wang, S., Liu, J., Fagan, M. B., and Nunberg, J. H. (2001) *J. Virol.* **75,** 11146–11156
13. Cao, J., Bergeron, L., Helseth, E., Thali, M., Repke, H., and Sodroski, J. (1993) *J. Virol.* **67,** 2747–2755
14. Ji, H., Shu, W., Burling, F. T., Jiang, S., and Lu, M. (1999) *J. Virol.* **73,** 8578–8586
15. Bar, S., and Alizon, M. (2004) *J. Virol.* **78,** 811–820
16. Mo, H., Konstantinidis, A. K., Stewart, K. D., Dekhtyar, T., Ng, T., Swift, K., Matayoshi, E. D., Kati, W., Kohlbrenner, W., and Molla, A. (2004) *Virology* **329,** 319–327
17. Edelhoch, H. (1967) *Biochemistry* **6,** 1948–1954
18. Johnson, M. L., Correia, J. J., Yphantis, D. A., and Halvorson, H. R. (1981) *Biophys. J.* **36,** 575–588
19. Fersht, A. (1999) in *Structure and Mechanism in Protein Science* (Julet, M., ed) pp. 508–539, W. H. Freeman and Company, New York
20. Yang, Z. N., Mueser, T. C., Kaufman, J., Stahl, S. J., Wingfield, P. T., and Hyde, C. C. (1999) *J. Struct. Biol.* **126,** 131–144
21. Lu, M., Ji, H., and Shen, S. (1999) *J. Virol.* **73,** 4433–4438
22. Thomas, S. T., Loladze, V. V., and Makhatadze, G. I. (2001) *Proc. Natl. Acad. Sci. U. S. A.* **98,** 10670–10675
23. Gallo, S. A., Finnegan, C. M., Viard, M., Raviv, Y., Dimitrov, A., Rawat, S. S., Puri, A., Durell, S., and Blumenthal, R. (2003) *Biochim. Biophys. Acta* **1614,** 36–50
24. Greenberg, M., Cammack, N., Salgo, M., and Smiley, L. (2004) *Rev. Med. Virol.* **14,** 321–337
25. Greenberg, M. L., and Cammack, N. (2004) *J. Antimicrob. Chemother.* **54,** 333–340
26. Lu, J., Sista, P., Giguel, F., Greenberg, M., and Kuritzkes, D. R. (2004) *J. Virol.* **78,** 4628–4637
27. Scales, S. J., Yoo, B. Y., and Scheller, R. H. (2001) *Proc. Natl. Acad. Sci. U. S. A.* **98,** 14262–14267
28. Eckert, D. M., Malashkevich, V. N., and Kim, P. S. (1998) *J. Mol. Biol.* **284,** 859–865
29. Knappenberger, J. A., Smith, J. E., Thorpe, S. H., Zitzewitz, J. A., and Matthews, C. R. (2002) *J. Mol. Biol.* **321,** 1–6